Strain effect on lattice vibration, heat capacity, and thermal conductivity of graphene

F. Ma,[1] H. B. Zheng,[1] Y. J. Sun,[1] D. Yang,[1] K. W. Xu,[1,2,a)] and Paul K. Chu[3,a)]
[1]*State Key Laboratory for Mechanical Behavior of Materials, Xi'an Jiaotong University, Xi'an 710049, Shaanxi, China*
[2]*Department of Physics and Opt-electronic Engineering, Xi'an University of Arts and Science, Xi'an 710065, Shaanxi, China*
[3]*Department of Physics and Materials Science, City University of Hong Kong, Tat Chee Avenue, Kowloon, Hong Kong, China*

(Received 17 July 2012; accepted 28 August 2012; published online 11 September 2012)

First-principle calculation based on density functional theory is performed to study the lattice vibration, heat capacity, and thermal conductivity of graphene under strain. Two degenerate optical branches in the phonon dispersion curves split near the G points due to the reduced crystal symmetry, and the frequencies of the optical phonon modes shift down thus inducing more phonon modes at a given temperature. The heat capacity is increased, but the thermal conductivity is reduced because of enhanced Umklapp scattering among more phonons. This phenomenon should be considered when determining the heat management of graphene-based devices. © *2012 American Institute of Physics*. [http://dx.doi.org/10.1063/1.4752010]

As integrated circuit dimensions enter the nanometer regime, silicon-based devices are approaching the performance limit[1] and other materials are being explored. In the graphene structure, there is an unpaired electron on each C atom that can travel freely along the plane. This leads to extremely high electron mobility of 10^5 cm^2/Vs,[2–4] which is much better than that of single-crystal silicon (1400 cm^2/Vs). Hence, graphene has been suggested to be a potential candidate to replace silicon in nanoelectronics, especially high-frequency devices.[1] The ultra-thin graphene layer bodes well for high-density integration, but the heat produced during device operation may affect the stability and reliability of the devices. As a two-dimensional structure, graphene is expected to exhibit phonon dispersion different from that of bulk materials and consequently possess unique thermal properties.

Theoretical and experimental investigations have demonstrated that similar to the electronic properties, the thermal properties of graphene is extremely sensitive to the feature size as well as local atomic configuration at the edges. For instance, the low-frequency branches may shift up with decreasing ribbon width due to the phonon confinement effect. As a result, the heat capacity increases[5] while the thermal conductivity decreases.[6,7] Zigzag graphene nanoribbons have higher thermal conductivity than armchair ones because the low-frequency bands of the former are more dispersive thereby accounting for the anisotropy in thermal conductance.[8] Jiang *et al.*[9] found by molecular dynamics simulation with quantum correction that isotopic doping reduced the thermal conductivity effectively in the slightly doped region, and it was not as transparent as in the highly doped region. Wang *et al.*[10] experimentally measured the thermal conductivity of the suspended and supported graphene using a thermal-bridge configuration and found that the room-temperature thermal conductivity of larger flakes was comparable to that of bulk graphite, but it diminished significantly in smaller flakes. It was further reduced in the supported samples because of phonon-boundary scattering at the graphene-contact interfaces. In addition to enhanced interface scattering, thermal misfit induced lattice strain may be dominant in the system if the negative thermal expansion coefficient of graphene is taken into account. In the nonharmonic region, the stretched lattice reduces the force constant softening the vibration frequency. Consequently, the thermal properties may change. In the work reported in this paper, first-principle method is used to calculate the lattice vibration phonon dispersion and density of states (DOS) of graphene under uniaxial strain along the zigzag direction. Our objective is to elucidate the physical nature as well as the dominant factors affecting the thermal properties of two-dimensional materials by focusing on the strain effect.

Graphene, one of the typical two-dimensional honeycomb crystals, has a space group of P6_3mc with lattice constants $a = b = 2.4656$ Å,[11] as shown in Fig. 1(a). The unit cell is indicated by the red parallelogram with two basic vectors, a1 and a2. Armchair and zigzag are the two typical configurations of graphene along the directions parallel or perpendicular to C–C bonds, respectively, as indicated by the X and Y axes. The two types of C–C bonds are denoted as bond 1 and bond 2. The layer separation is increased up to 25 Å, so that the interation between layers can be ignored. The

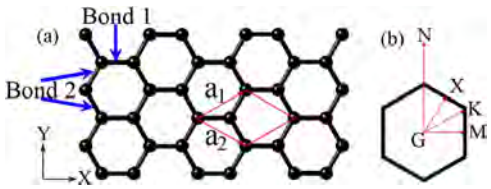

FIG. 1. (a) Graphene model in which the unit cell is indicated by a red parallelogram with a1 and a2 being the two basic vectors and (b) Corresponding reciprocal lattice with G, M, K, N, and X indicating the high-symmetry K points.

[a)]Authors to whom correspondence should be addressed. Electronic addresses: kwxu@mail.xjtu.edu.cn and paul.chu@cityu.edu.hk.

periodic boundary conditions are applied to all the three directions. With regard to the phonon dispersion, the high-symmetry points are selected deliberately as shown in the first Brillouin zone in Fig. 1(b). The crystal symmetry and reciprocal lattice are changed under strain, depending on the strain direction. For the ideal graphene, G, M, and K are selected to calculate the phonon dispersion, while G, N, and M are for the strain along the zigzag direction. The strain is exerted by changing the lattice constant along a given direction and relaxing the atom position in the perpendicular direction.[12]

The generalized gradient approximation with the Perdew-Burke-Ernzerhof exchange-correlation potential (GGA-PBE) with a kinetic-energy cutoff of 400 eV is adopted. The convergence of the total energy is chosen to be 1.0×10^{-7} eV, and structure optimization is performed until the force acting on each atom is less than 0.001 eV/Å.[8] The maximum iteration number is 100, and the mesh grid separation is 0.1 $Å^{-1}$. Supercells of $8 \times 8 \times 1$ and $3 \times 5 \times 1$ are utilized to calculate the phonon dispersion curves and density of states of graphene with or without uniaxial strain along the zigzag direction [Fig. 1(a)]. After the phonon spectrum is obtained, the heat capacity can be calculated using the phonon density of states $g(\omega)$ as shown in the following[13]:

$$Cv(T) = k_B \int_0^{\infty} \frac{(\hbar\omega/k_BT)^2 \exp(\hbar\omega/k_BT)}{[\exp(\hbar\omega/k_BT) - 1]^2} g(\omega) d\omega, \quad (1)$$

where k_B and $\hbar$ are Boltzmann and Planck constants, respectively. The thermal conductivity is calculated as[14]

$$k = \frac{1}{4\pi k_B T^2 h} \sum_{s=1\ldots i} \int_{q_{\min}}^{q_{\max}} \left\{ [\hbar^2 \omega_s(q)^2 v_s(q)^2 \tau_{tot}(s,q)] \times \frac{\exp[\hbar\omega_s(q)/k_BT]}{[\exp\left(\hbar\omega_s(q)/k_BT\right) - 1]^2} q \right\} dq, \quad (2)$$

where $h = 0.355$ nm is the graphene thickness. Two scattering mechanisms are involved, that is, three-phonon Umklapp scattering[14] and edge scattering[15]

$$\tau_U(s,q) = \frac{1}{\gamma_s^2} \frac{M v_s^2}{k_B T} \frac{\omega_{s,\max}}{\omega^2}, \quad (3)$$

$$\frac{1}{\tau_B(s,q)} = \frac{v_s}{d} \frac{1-p}{1+p}, \quad (4)$$

$$\frac{1}{\tau_{tot}(s,q)} = \frac{1}{\tau_U(s,q)} + \frac{1}{\tau_B(s,q)}, \quad (5)$$

where v_s and $\omega_{s,\max}$ are, respectively, the average phonon velocity and maximum cut-off frequency of a given branch, M is the mass of a primitive unit cell, γ_s is the mode-dependent Gruneisen parameter and selected to be 1.11,[15] d is the width of the graphene flake, and p is the specularity coefficient depending on the edge roughness.

Figs. 2(a) and 2(e) display the phonon dispersion curves and DOS of ideal graphene without strain, respectively. Six branches can be observed from Fig. 2(a). Three of them are the optical phonon branches (LO, TO, and ZO) having higher frequencies, whereas the other three are the acoustical phonon braches (LA, TA, and ZA). The maximum phonon frequency at the G point is 47.023 THz (1569 cm^{-1}) and the frequency of the ZO branch at the G point is 26.147 THz (872 cm^{-1}). They are very close to the experimental values of 1582 cm^{-1} and 868 cm^{-1}, respectively.[16] This demonstrates the validity of the theoretical calculation. Figs. 2(b)–2(d) depict the phonon dispersion curves of graphene under uniaxial strain of 8%, 16%, and 23% along the zigzag direction and the corresponding DOS is shown in Figs. 2(f)–2(h).

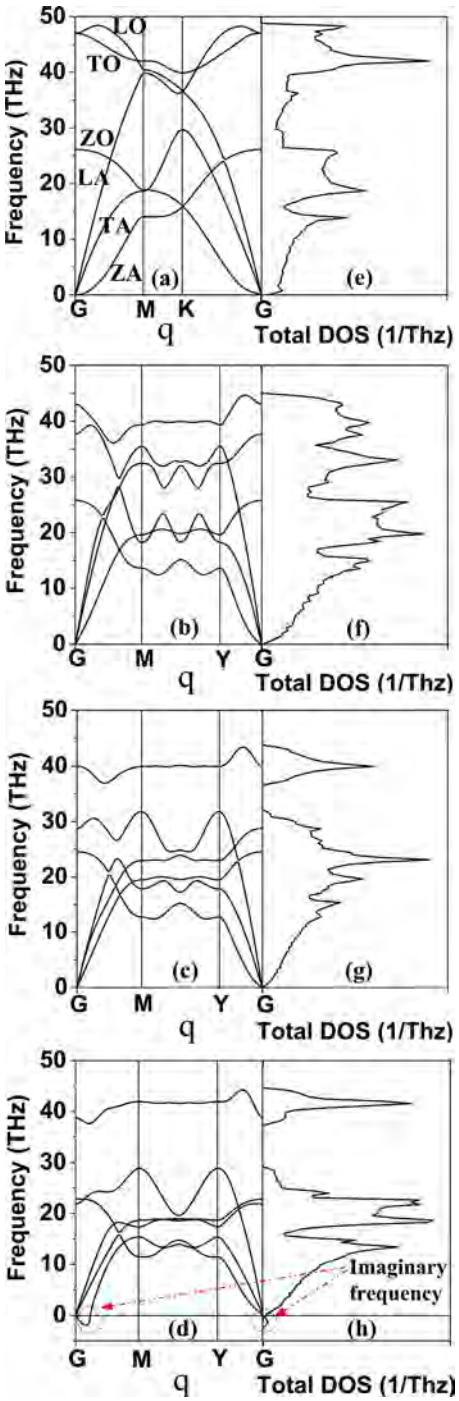

FIG. 2. Phonon dispersion curves of graphene under typical uniaxial strain of (a) 0%, (b) 8%, (c) 16%, and (d) 23% along the zigzag direction, and (e), (f), (g), and (h) corresponding total density of states.

The two degenerate optical branches split near the G points due to the reduced crystal symmetry in the presence of lattice strain and the split becomes more evident at a larger strain. This results in a frequency gap of about 10 THz near 35 THz at a strain of about 16%, as shown in Figs. 2(c) and 2(g). Gunawardana *et al.* have also reported this strain induced band gap in graphene nanoribbons.[17] It implies that the vibration modes in the frequency region are forbidden, similar to the band gap in electronic crystals and photonic crystals. This can be utilized in the applications such as thermal rectifiers,[18] thermal transistors,[19] and thermal memories,[20] but further investigation is required. When the strain is increased up to 23%, imaginary frequencies appear near the G points as indicated by the red arrows in Figs. 2(d) and 2(h). The structure becomes unstable and the phonon modes are softened. Similar results are obtained when the strain is along the armchair direction, but the instability appears at 20% strain. In fact, when the uniaxial strain is applied along the armchair direction, the tensile force is mainly borne by the C–C bonds parallel to the stress and only bond stretching occurs. When the stress is not parallel to the C–C bonds in the case of loading along the zigzag direction, both bond rotation and stretching are involved, and hence fracture is slightly more difficult in the latter case.[21]

Fig. 3 displays the variation in the frequencies at the G point for the LO and TO phonon braches and characteristic bonds with applied strain. The Ag (R) mode at the G point is induced due to the reverse movement of the nearest C atoms parallel to bond 1, whereas the B1g (R) mode is caused by the reverse movement perpendicular to bond 1 [Fig. 1(a)]. Although the bond length of bond 1 changes a little, the length of bond 2 increases significantly with the applied strain [Fig. 3(b)]. As shown in Fig. 3(a), the frequency of the B1g (R) mode shifts down faster with applied strain than the Ag (R) mode. It can be found by comparing Figs. 3(a) and 3(b) that the length variation of bond 2 and frequency shift of B1g(R) are directly related. Therefore, the rapid frequency shift of the B1g(R) mode should be induced by the change of bond 2. The force constant is reduced as a result of the increased C–C bond length upon stretching and the optical phonon modes are softened, as presented in Fig. 2.

The altered frequencies affect the heat capacity and thermal conductivity. Fig. 4 plots the calculated results of these two thermal parameters according to Eqs. (1)–(5). As shown

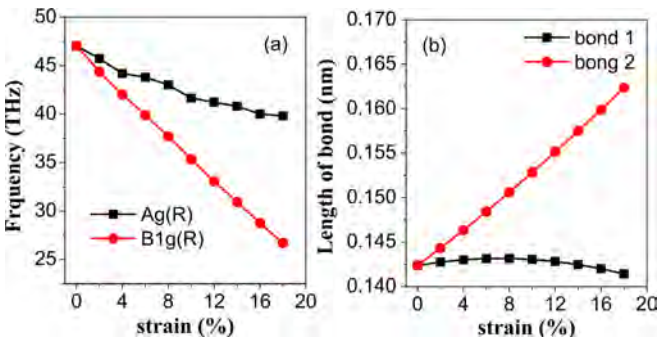

FIG. 3. (a) Frequency shift of the two high-frequency modes at the G points, Ag(R), and B1g(R) of graphene in the presence of uniaxial strain along the zigzag direction and (b) bond length variation of two typical C–C bonds, bond 1 and bond 2.

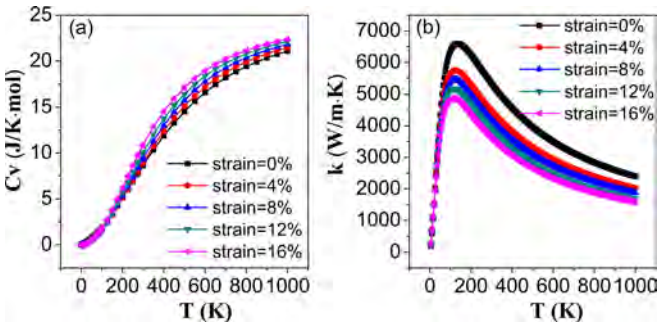

FIG. 4. (a) Heat capacity and thermal conductivity of graphene under uniaxial strain as a function of temperature.

in Fig. 4(a), the heat capacity increases with temperature because there are more phonons. At a given temperature, the strain along the zigzag direction may cause the frequency to shift down. More phonons are activated and the heat capacity which depends on temperature increases. At a temperature below 200 K, the strain effect is less evident because most of the phonons activated at the low temperature are low-frequency ones, but those with discernible frequency shift under strian is mainly the high-frequency ones. However, this is not the case at a high temperature when more high-frequency modes are involoved and the strain effect becomes significant. Fig. 4(b) shows the thermal conductivity of 3 μm wide graphene under strain. The trend is preserved. That is, the thermal conductivity increases with temperature initially and then decreases. At a given temperature, for example, 300 K, the strain pares the thermal conductivity. On one hand, the strain usually reduces the crystal symmetry of graphene and may enhance phonon scattering, on the other hand, the phonon modes shift down to lower frequencies. Consequently, more phonons are activated and the Umklapp scattering effect should be more prominent. The thermal conductivity is reduced in the presence of an applied strain, especially at a high temperature.[22] The variation of thermal conductivity with applied strain is different from that reported by Zhai *et al.*[23] In their work[23] based on the nonequilibrium Green's function method, they calculate the thermal transport properties of graphene under homogeneous uniaxial strain and remarkable enhancement of thermal conductivity up to 36% is obtained. The thermal conductance obtained by them is ballistic. That is, the mean free path is much larger than the size of the graphene nanoribbons, and defect scattering and phonon Umklapp scattering are not involved. Hence, the thermal carrier role of the increased phonons is only considered. However, at room temperature or above, Umklapp scattering among phonons is dominant,[15] and it will decrease the thermal conductivity with tensile strain, as stated in the letter. So strain engineering may provide us a candidate method to modify the thermal properties of graphene. However, experimental investigations are required to confirm the the results.

In summary, first-principle calculation is performed to study the strain effect on the phonon dispersion curves and thermal properties of graphene. Two degenerate optical dispersion branches (LO and TO) split at the G points in the prsence of strain due to the reduced crystal symmetry, and a frequecny gap of about 10 THZ appears. This is similar to the bandgap of electronic and photonic crystals and may be

utilized in the applications of phonon modulated devices. The strain also downshifts the frequencies of the optical phonon modes. In this case, more phonon modes are activated at a given temperature. The heat capacity increases, but the thermal conductivity diminishes because of enhanced Umkapp scattering. The results are uesful to the design of carbon-based nanoelectronic devices.

This work was jointly supported by Key Project of Chinese National Programs for Fundamental Research and Development (Grant No. 2010CB631002), National Natural Science Foundation of China (Grant Nos. 51271139 and 51171145), National Ministries and Commissions (Grant No. 6139802-04), New Century Excellent Talents in University (NCET-10-0679), Fundamental Research Funds for the Central Universities, and Hong Kong Research Grants Council (RGC) General Research Funds (GRF) No. CityU 112510.

[1]M. Leong, B. Doris, J. Kedzierski, K. Rim, and M. Yang, Science **306**, 2057 (2004).
[2]K. S. Novoselov, A. K. Geim, S. V. Morozov, D. Jiang, M. I. Katsnelson, I. V. Grigorieva, S. V. Dubonos, and A. A. Firsov, Nature (London) **438**, 197 (2005).
[3]Y. Zhang, Y. W. Tan, H. L. Stormer, and P. Kim, Nature (London) **438**, 201 (2005).
[4]S. V. Morozov, K. S. Novoselov, M. I. Katsnelson, F. Schedin, D. C. Elias, J. A. Jaszczak, and A. K. Geim. Phys. Rev. Lett. **100**, 016602 (2008).
[5]W. Liang, Y. Xiao, and J. W. Ding. Acta Phys. Sin. **57**, 3714 (2008), available at: http://wulixb.iphy.ac.cn/EN/abstract/abstract14330.shtml.
[6]E. Muñoz, J. X. Lu, and B. I. Yakobson, Nano Lett. **10**, 1652 (2010).
[7]Z. Huang, T. S. Fisher, and J. Y. Murthy, J. Appl. Phys. **108**, 094319 (2010).
[8]Z. W. Tan, J. S. Wang, and C. K. Gan, Nano Lett. **11**, 214 (2011).
[9]J. W. Jiang, J. H. Lan, J. S. Wang, and B. W. Li, J. Appl. Phys. **107**, 054314 (2010).
[10]Z. Q. Wang, R. G. Xie, C. T. Bui, D. Liu, X. X. Ni, B. W. Li, and J. T. L. Thong, Nano Lett. **11**, 113 (2011).
[11]R. Gillen, M. Mohr, C. Thomsen, and J. Maultzsch. Phys. Rev. B **80**, 155418 (2009).
[12]F. Liu, P. B. Ming, and J. Li. Phys. Rev. B **76**, 064120 (2007).
[13]J. Hone, Top. Appl. Phys. **80**, 273 (2001).
[14]D. L. Nika, S. Ghosh, E. P. Pokatilov, and A. A. Balandin, Appl. Phys. Lett. **94**, 203103 (2009).
[15]D. L. Nika, E. P. Pokatilov. A. S. Askerov, and A. A. Balandin, Phys. Rev. B **79**, 155413 (2009).
[16]R. J. Nemanich, G. Lucovsky, and S. A. Solin. Mater. Sci. Eng. **31**, 157 (1977).
[17]K. G. S. H. Gunawardana, K. Mullen, J. Hu, Y. P. Chen, and X. Ruan, Phys. Rev. B **85**, 245417 (2012).
[18]M. Terraneo, M. Peyrard, and G. Casati, Phys. Rev. Lett. **88**, 094302 (2002).
[19]B. Li, L. Wang, and G. Casati, Appl. Phys. Lett. **88**, 143501 (2006).
[20]L. Wang and B. Li, Phys. Rev. Lett. **101**, 267203 (2008).
[21]H. Zhao, K. Min, and N. R. Aluru. Nano Lett. **9**, 3012 (2009).
[22]N. Wei, L. Q. Xu, H. Q. Wang, and J. C. Zheng. Nanotechnology **22**, 105705 (2011).
[23]X. Zhai and G. Jin, Europhys. Lett. **96**, 16002 (2011).